Seismic Motion Detection and Classification Methodology for Buildings Using DFT and SVM

Ernesto A. Taypicahuana Loza
Instituto Nacional de Investigación y Capacitación en Telecomunicación
Universidad Nacional de Ingeniería
etaypicahuana@inictel-uni.edu.pe

Antero Castro Nieto
Instituto Nacional de Investigación y Capacitación en Telecomunicación
Universidad Nacional de Ingeniería
acastro@inictel-uni.edu.pe

Samuel G. Huaman Bustamante
Instituto Nacional de Investigación y Capacitación en Telecomunicación
Universidad Nacional de Ingeniería
shuaman@inictel-uni.edu.pe

2023 Argentine Conference on Electronics (CAE) | 979-8-3503-9954-7/23/$31.00 ©2023 IEEE | DOI: 10.1109/CAE56623.2023.10087012

***Abstract*— Analyzing the acceleration signals of buildings during a seismic event helps us to identify the vibrational intensity of the structure. This research proposes a methodology to recognize the level of the vibrational intensity of a building during an earthquake with a few seconds before its maximum vibration using the P wave response. The proposed methodology is based on the Discrete Fourier Transform (DFT) and Support Vector Machine (SVM). This methodology results in an alert level that is classified according to its vibrational intensity (low, moderate and high). Each building could have different alerts in the event of an earthquake since may have different natural frequencies. A prototype implemented with a Raspberry Pi V4 B embedded system, two acceleration sensors called MPU6050 based on MEMS and a Wi-Fi antenna, mainly, is used. Also, filters were used to attenuate noise. The STA/LTA algorithm is used to compare the detection time. The results show that it is convenient to use the methodology for two main reasons. Firstly, this uses one tenth of the samples needed in the STA/LTA algorithm for detection and with the same efficiency. Secondly, the classification of the alert level in the building has a correlation greater than 0.8 with the PGA of the seismic signal that occurred in its structure.**

Keywords—accelerometer, resonance in building, structural health monitoring, early earthquake warning

I. Introduction

According to the United Nations, an early warning system uses integrated systems in order to prepare the population for a natural disaster and thus try to safeguard human life. One of the applications of early warning systems is the early warning of an earthquake, since each year more than 1000 earthquakes of magnitude greater than 5 points on the Richter scale are recorded worldwide [1]. The most affected countries are those located in the ring of fire.

Nowadays, with the appearance of new technology and due to the large number of seismic events that occur annually, better earthquake early warning (EEW) systems are being developed. These systems are important because their proper use can warn the population of an imminent seismic event. For the detection of these events, the systems mainly use accelerometers, since these are devices capable of detecting vibrations. There are several ways to implement it, such as the ShakeAlert system [2], which uses cell phone accelerometers through a mobile application, this research proposes to create a network to notify users of a seismic event. Another way is using the accelerometric stations with algorithms as in [3] to detect the earthquake with some anticipation; furthermore, they implement their own prototype with MEMS (Microelectromechanical systems) accelerometers [4] to carry out the same application, but with low-cost devices.

In this research, we proposed a methodology to detect and classify the vibration intensity of the building, which consists of extracting the characteristics related to the maximum value of the spectral power density of the acceleration signal generated for an earthquake in buildings and classify these characteristics using the SVM (Support Vector Machine) technique [5] aiming to generate an alert. The alert is classified in three levels: level 1 represents slight vibration, level 2 represents moderate vibration and level 3 represents high vibration. Additionally, we use STA/LTA (Short Time Average over Long Time Average) algorithm [6] to compare results.

Using the background seen in [7] and [8], a prototype is implemented with the triaxial sensor MPU-6050 [9] based on MEMS and the Raspberry Pi V3 B+ [10]. The sensor samples the acceleration signals in three axis and the embedded system processes them. This prototype is installed on the ceiling of top floor of a building since it presents higher accelerations as indicated in [11]. This paper contains three sections: Development of the methodology, Results and Conclusion.

II. Development of the Methodology

The methodology is explained in five sub-section that contain information on the generation dataset to simulation seismic effect on buildings, features, classifier model, implementation of hardware and algorithms.

A. Dataset Generation of Simulated Earthquakes in Building

Seismic signals extracted from [12] were sampled with frequency of 200 Hz and these are analyzed before using in the simulation of buildings motion. For instances, Table I indicates the magnitude, date and place of each earthquake in Peru and Table II shows the characteristics of each signal evaluating the Peak ground acceleration (PGA) and range in cm/s^2.

TABLE I.
Earthquake Data

Earthquake Magnitude	***Date***	***Place***
3.6	13/02/2018	Lima, 6 km Sur de Tamoraque
5.3	11/04/2019	Ica, 34 km Sur-Oeste de Pisco
7.2	26/05/2019	Lorte, 70 km Sur-Este de Lagunas

TABLE II.
MAIN FEATURES OF EARTHQUAKE DATA

Earthquake Magnitude	*PGA Este* (cm/s^2)	*PGA Norte* (cm/s^2)	*PGA Z* (cm/s^2)	*Range* (cm/s^2)
3.6	-1.98	-2.13	-0.74	-2 a 2
5.3	10.58	-12.2	-6.41	-10 a 10
7.2	-81.08	75.98	67.55	-50 a 50

In this work, a slice of P-wave from the whole seismic signal is used, since, when an earthquake occurs, these waves arrive first to sensors. This way it is possible to detect and classify the earthquake in a short time before damages happen. In Table III is showed the mean, standard deviation (S.D.), and PGA of the P-wave of the earthquakes, mentioned in Table I, for each magnitude and direction.

TABLE III.
MAIN FEATURES OF P-WAVE SIGNAL

Earthquake Magnitude	*Feature*	*Este*	*Norte*	*Z*
3.6	Mean (cm/s^2)	0.0012	-0.0041	-0.0058
	S.D.(cm/s^2)	0.0895	0.2837	0.2279
	PGA (cm/s^2)	-0.2848	-0.9234	-0.6934
5.4	Mean (cm/s^2)	0.0033	0.0004	-0.0023
	S.D.(cm/s^2)	1.0284	0.6144	0.5795
	PGA (cm/s^2)	-3.8988	2.3605	-1.8750
7.2	Mean (cm/s^2)	0.0084	-0.0103	-0.0102
	S.D.(cm/s^2)	5.6423	1.8593	1.9645
	PGA (cm/s^2)	20.9687	5.6944	-7.6572

The building acceleration dataset is generated by simulation. For this purpose, CAD designs of the building models with different characteristics in floors, height of each floor, number of rooms per floor is carried out. These variants were taken into account to design 48 buildings in SolidWorks software (trial) [13]. Each building has different natural frequencies.

A transient analysis is performed in ANSYS software (trial) with the P-wave slices to obtain the resonances of the buildings caused by the earthquakes. The dynamic response is produced with numerical methods step by step as indicated in [14]. As a result, 144 signals or slices are obtained, each one has a duration between 9 and 10 seconds. Fig. 1 shows a seismic signal extracted from [12], the P wave of the seismic signal, the dynamic response of the building and the spectrogram of the signal by one-second windows for frequencies between 0 and 20 Hz. The signal must be grouped in slices so that the algorithm detects and classifies with a small number of samples. In the spectrogram, it is observed that the frequencies around the natural frequency of the building have higher power in decibels before a seismic event. Each slice contains 200 samples so the algorithm only needs one second to give a result. If the result indicates 0, then there was no earthquake; if it indicates a number other than 0, then there is a resonance in the building. The resonance level in the building is classified as 1, 2 or 3; where 3 is the highest level. In total there is a bunch of 1296 events containing 200 samples each, with their respective target.

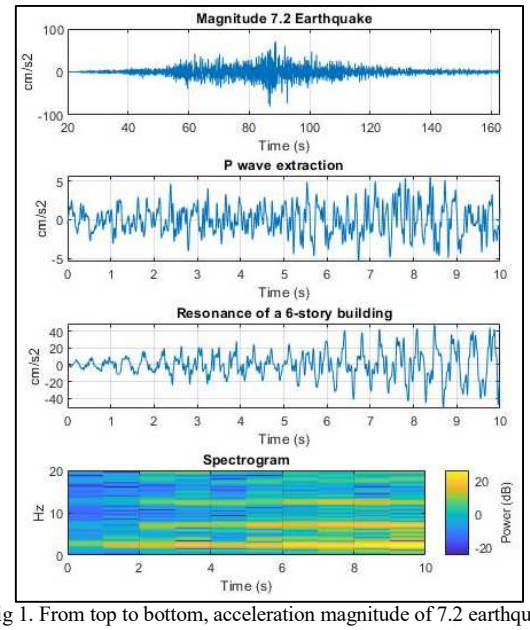

Fig 1. From top to bottom, acceleration magnitude of 7.2 earthquake, P-wave extraction, Dynamic response to P-wave of a 6-story building, seismic response spectrogram.

The intensity of acceleration increases according to the height of the building [11], so the first and last floors are important to know the variation of the amplitudes generated in the building. In addition, it is analyzed in the axial directions of the buildings because they present the greatest force generated by the vibration of the structure and are also it can be the most frequent cause of its collapse [11]. The simulation result focuses on the acceleration signals because direct measurement is not possible in other features.

B. *Features*

In Table IV are shown statistical characteristics, intensity of Arias [15] and features related to frequency. The last one, is proposed to extract characteristics related to seismic resonance in buildings, for which the maximum power in decibels is used for frequencies greater than or equal to 1 Hz and less than or equal to 15 Hz of its power spectral density (PSD). This interval is important since natural frequencies of buildings are between those values [16]. These characteristics are calculated from the acceleration vector described in (1). Then, the Discrete Fourier Transform (DFT) [17] is calculated, up to frequencies less than or equal to 15 Hz as indicated in equation (2). Finally, equation (4) is the maximum value of vector (3) in decibels. These proposed features are presented in Table IV as u19, u20, u21 and u22.

$$a = [a_1; a_2; a_3; \dots; a_{100}] \tag{1}$$

$$\begin{cases} A_1 = \frac{2}{100}\sum_{k=1}^{100} a_k * \left(cos\left(\frac{2\pi k(0)}{100}\right) - isen\left(\frac{2\pi k(0)}{100}\right)\right) \\ A_2 = \frac{2}{100}\sum_{k=1}^{100} a_k * \left(cos\left(\frac{2\pi k(1)}{100}\right) - isen\left(\frac{2\pi k(1)}{100}\right)\right) \\ \vdots \\ A_{15} = \frac{2}{100}\sum_{k=1}^{100} a_k * \left(cos\left(\frac{2\pi k(15)}{100}\right) - isen\left(\frac{2\pi k(15)}{100}\right)\right) \end{cases} \tag{2}$$

$$A = [A_1; A_2; A_3; \dots; A_{15}] \tag{3}$$

$$u = 20\log_{10}(\max(|A|)) \tag{4}$$

TABLE IV.
EXTRACTED FEATURES

ui	*Description*
u1	Variance of north axis signal of the first floor
u2	RMS value of north axis signal of the first floor
u3	Interquartile range of north axis signal of the first floor
u4	Arias intensity of north axis signal of the first floor
u5	Variance of east axis signal of the first floor
u6	RMS value of east axis signal of the first floor
u7	Interquartile range of east axis signal of the first floor
u8	Arias intensity of east axis signal of the first floor
u9	Average value of the acceleration modulus of the first floor
u10	Variance of north axis signal of the last floor
u11	RMS value of north axis signal of the last floor
u12	Interquartile range of north axis signal of the last floor
u13	Arias intensity of north axis signal of the last floor
u14	Variance of east axis signal of the last floor
u15	RMS value of east axis signal of the last floor
u16	Interquartile range of east axis signal of the last floor
u17	Arias intensity of east axis signal of the last floor
u18	Average value of the acceleration modulus of the last floor
u19	Maximum power in decibels of the power spectral density for frequencies below 15 Hz in the North direction of the first floor
u20	Maximum power in decibels of the power spectral density for frequencies below 15 Hz in the East direction of the first floor
u21	Maximum power in decibels of the power spectral density for frequencies below 15 Hz in the North direction of the last floor
u22	Maximum power in decibels of the power spectral density for frequencies below 15 Hz in the East direction of the last floor

In the correlation matrix shown in Fig. 2, it is observed that the features u19, u20, u21 and u22 have a high correlation with respect to the magnitude of the earthquake, which indicates that it is advisable to work with these features. However, measuring the accelerations of the first floor require accurate instruments, because lower amplitudes require a higher acquisition resolution [11]. Therefore, the classifier will be designed with respect to the accelerations of the last floor. Also, this classifier was analyzed with the characteristics u9 and u18 which have a correlation greater than 0.7; however, greater separability in the data was not achieved.

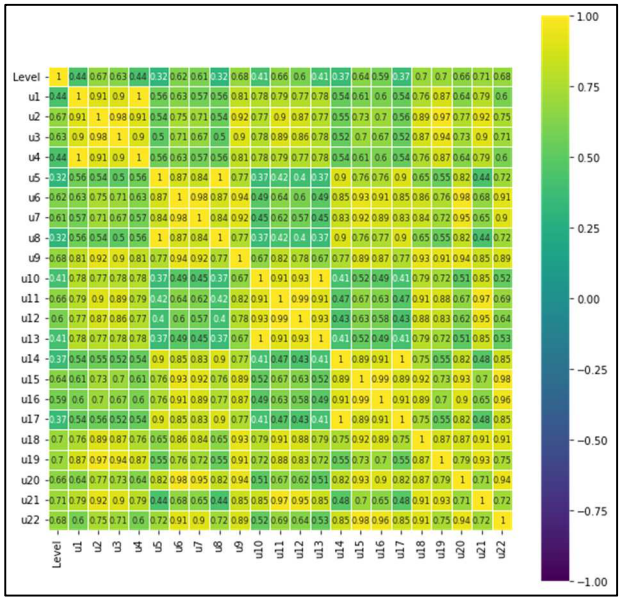

Fig 2. Correlation Matrix of the extracted features.

Hereafter, the features selected for the classifier will be called z1 and z2 (u21 and u22). The Fig. 3(a) shows the box plot of the features z1 and z2, which have a slight skew towards positive values. The statistical descriptors of the features are presented in Table V. It is highlighted that the minimum value between them would be approximately -25 dB, hence, it is necessary to consider this value to design the prototype and the classifier. The scatter plots, shown in Fig. 3(b), can be seen the features and its histograms. This last one presents Gaussian distribution.

TABLE V.
STATISTICAL CHARACTERISTICS

Earthquake Magnitude	*Z1*	*Z2*
Mean	10.597717	9.107898
Std	14.308202	15.347335
min	-20.003680	-24.490265
25%	-2.374138	-5.385359
50%	13.944077	11.605844
75%	21.968592	21.350496
max	39.403973	41.185884

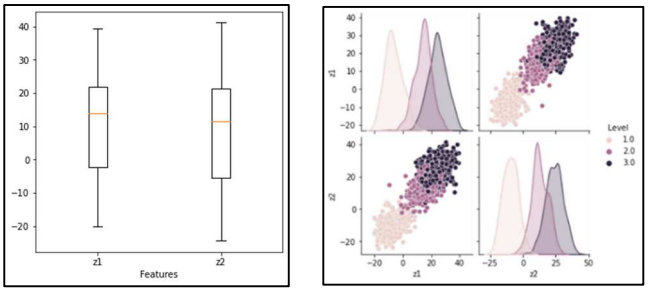

(a) (b)

Fig 3. (a) Box plot of the features. (b) Scatter plot and histograms.

C. *Classifier Design*

Before designing the classifier, noise is added to the signals to becoming realistic. The classifier can generalize and discriminate even with a certain level of noise in the signal. The noise presented in Fig. 4 is modeled considering the minimum value of the box plot shown in Fig. 3 (a), so it is proposed the constraint of equation (5).

$$z_{noise} < -27 \qquad (5)$$

To get this constraint, white noise with Gauss distribution is chosen, using media 0 and standard deviation equal to 0.2.

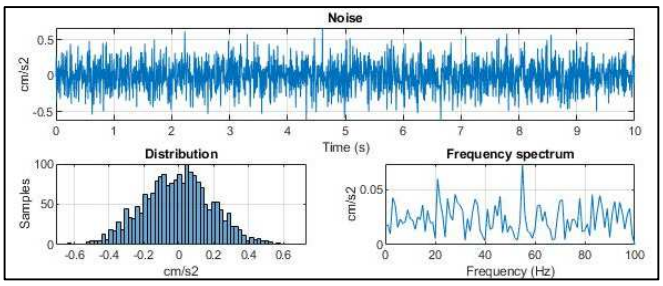

Fig 4. White noise with mean 0 and standard deviation 0.2.

Then, a Support Vector Machine (SVM) based classifier is configured and trained [5]. To train this classifier we use cross-validation [18] to avoid over-fitting. It is separated into 4 groups and in each iteration the precision and sensitivity are evaluated; these results are presented in Table VI. The performance evaluation is shown in the confusion matrix presented in Fig. 5(a), with an accuracy of 0.888199 andF1_score of 0.882239.

TABLE VI.
TRAINING EVALUATION

Iteration	*MSE*	*R2*
1	0.142361	0.7754407
2	0.107639	0.8349112
3	0.107639	0.8446115
4	0.100694	0.8525814

For inference, the following functions shown in equations (10), (11) and (12) are programmed in an embedded system. It must be taken into account that the characteristics of the vector Z shown in equation (6) must first be calculated. The coefficients of the separation of the characteristics z1 and z2 are shown in equations (7), (8) and (9). The graph z1 vs z2 presented in Fig. 5(b), it can see the lines best separate the clusters to obtain an alarm level in case of an earthquake.

$$Z = [z_1, z_2]^T \tag{6}$$

$$W_1 = [-0.1964, -0.1495] \tag{7}$$

$$W_2 = [-0.1813, -0.3010] \tag{8}$$

$$W_3 = [-0.1372, -0.1550] \tag{9}$$

$$y_1 = W_1 * Z + 2.6364 \tag{10}$$

$$y_2 = \begin{cases} W_2 * Z + 0.9712, & y_1 < 0 \\ W_3 * Z + 5.4371, & y_1 \geq 0 \end{cases} \tag{11}$$

$$Clase = \begin{cases} 1, & y_2 < 0 \wedge y_1 < 0 \\ 2, & y_2 * y_1 < 0 \\ 3, & y_2 \geq 0 \wedge y_1 \geq 0 \end{cases} \tag{12}$$

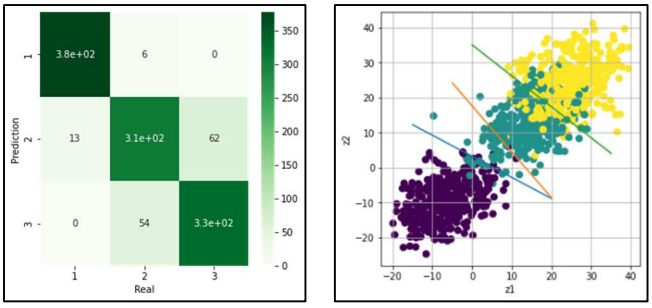

(a) (b)

Fig 5. (a) Confusion matrix. (b) Scatter plot.

D. Implemented Prototype and Signal Processing

The acquisition system of [19] is used, since in these experimental tests low total harmonic distortion (THD) and high signal noise ratio (SNR) are observed for developed methodology. According to the electrical and digital characteristics of the sensor, it is possible to use with the proposed method since, according to [9], it has a range of ±2000 cm/s^2, a sensitivity of 16384 LSB/g, a 16-bit Σ-Δ ADC and a spectral density of 400 µg/√Hz. This last parameter scaled to the processing units would be 0.4 mg/√Hz and -7.9588 dB, in terms of power. According to Fig. 5(b), the sensor can classify high and moderate level earthquakes without any problem, but some mildly earthquakes cannot be classified.

E. Programming of algorithms in the embedded system

The proposed method is mainly composed of two main algorithms. The first is the Discrete Fourier Transform (DFT), which is used to compute z1 and z2 for seismic motion detection and the second is the Support Vector Machine (SVM) which is used to classify the resonance intensity of the building. according to the values of z1 and z2. This classification has three levels, which can be related to an alarm type. Value 1 indicates low alarm, value 2 moderate alarm and value 3 high alarm. These algorithms together with the STA/LTA algorithm are calculated every time they capture a sample.

The execution of the algorithms is carried out as follows. First, the MPU6050 sensor is parameterized using the I2C protocol to display the acceleration signal with a frequency of 100 Hz and a range of ±2 g. Consecutively, the captured signal is scaled in units of cm/s^2 and the filters of [19] are applied. Next, the STA/LTA algorithm [6] is executed with a long window of 20 s and a short window of 2 s. At the same time, the proposed method is executed calculating the z1, z2 and the alarm. Finally, the results are saved consecutively. Fig. 6 shows the 5-minute acquisition, in which some perturbations were performed to observe the results of the STA/LTA and the proposed method. The execution of the embedded system program lasts approximately 5.4 ms, which is less than its sampling period (10 ms).

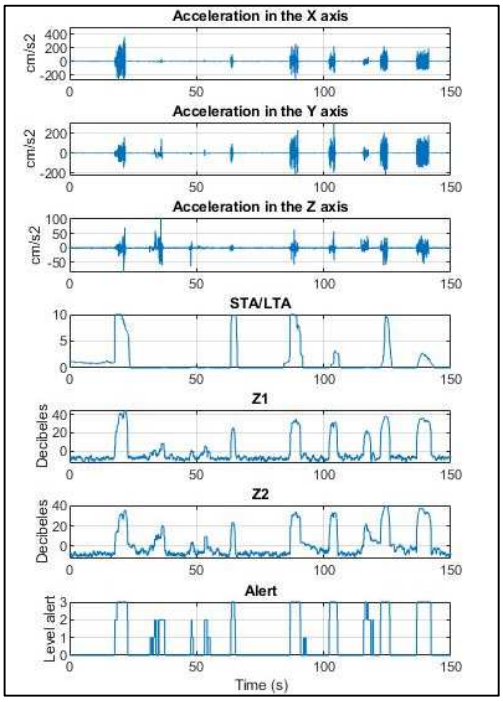

Fig 6. Acceleration signals in the X, Y and Z axis. STA/LTA algorithm. Proposed method.

III. Results

A seismic simulator [20] and a scale model of a structure are used for the evaluation of the detection and classification of the intensity of the resonance in the structure. The model is made of A36 steel and has a weight distributed of 56 kg in total. It has an impulse response around of 4.4 Hz and 11.8 Hz in X and Y axis, respectively. Various experimental tests were carried out with the vibrating table straight and rotated 45° respect to initial position as shown in Fig. 7, also various seismic signals of different intensities were set in the simulator. In total, 40 valid experimental trials were obtained for the analysis. In each of these, STA/LTA algorithm and the method proposed are introduced for the detection and classification of the vibrational intensity. The analysis of the detection, classification and computational cost of the algorithms are presented below.

(a)

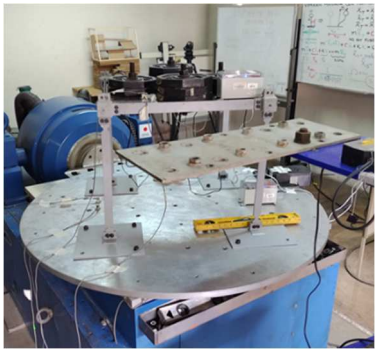

(b)

Fig 7. (a) Metallic scale structure. (b). Metallic structure rotated 45° with respect to the initial position.

A. Earthquake Detection Assessment

The detection time of the earthquake occurrence is evaluated in each experimental trial. A comparison is made with the STA/LTA algorithm for reference. In (13) and (14) the thresholds of each algorithm are indicated. The threshold of the STA/LTA algorithm is 3 and for the proposed method it is -2.0. If thresholds are exceeded, it means that a movement has occurred in the structure.

$$\frac{STA}{LTA} \geq 3.0 \tag{13}$$

$$z_1 \geq -2.0 \; or \; z_2 \geq -2.0 \tag{14}$$

The Fig. 8 shows the experimental trials from 1 to 40 on the X axis and the elapsed seconds from 1 to 70 on the Y axis. Each box represents one second. In each experimental trial, there are three boxes with different colors: red, orange and black. Red box represents detection by means of the proposed method; orange box, detection with the STA/LTA algorithm; and the black box, the maximum PGA in absolute value of the earthquake.

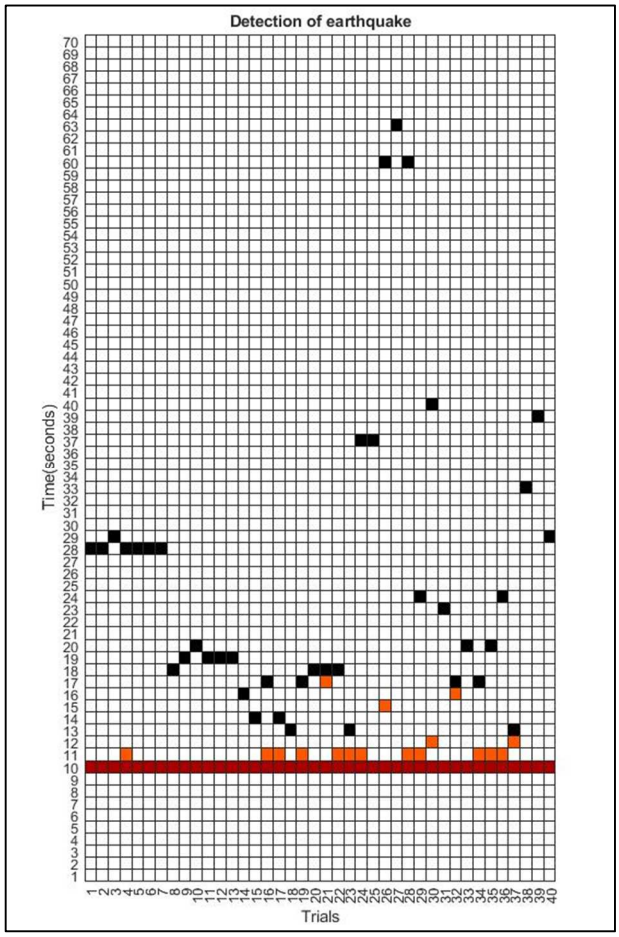

Fig 8. Motion detection in each experimental trial.

In Fig. 8 it is observed that in all the experimental tests, the detection time using the DFT algorithm (t_{DFT}) is minor or equal than the one using the STA/LTA algorithm ($t_{STA/LTA}$). Therefore, the relationship shown in (15) is deduced.

$$t_{STA/LTA} \geq t_{DFT} \tag{15}$$

B. Evaluation of Earthquake Alert Classification

After having detected the seismic response in the structure, it is processed a second later to identify the type of intensity through an alarm. In that second, z1 and z2 are calculated again. If the calculated z1 and z2 are greater than the previous ones, as indicated in (16), the type of intensity is classified, otherwise z1 and z2 are continuously recalculated until the detection is made again.

$$z_1(t_{DFT}+1) > z_1(t_{DFT}) \; and \; z_2(t_{DFT}+1) > z_2(t_{DFT}) \tag{16}$$

Fig. 9 shows the alerts obtained from the experimental trials versus their maximum absolute PGA values. This alert is obtained one second after the detection if the condition (16) is met. The PGA is observed to occur several seconds after detection. In Fig. 9 appears a separation between the alarm levels according to the maximum absolute PGA value, therefore, the evaluation of the correlation between them is important. A correlation of 0.886 was obtained among these values.

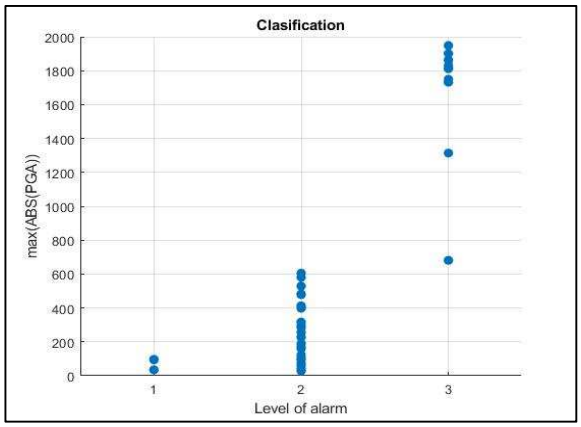

Fig 9. Relationship between the alert and the maximum value of the absolute value of the PGA presented in the seismic signals.

C. Computational Cost

An embedded system called Raspberry Pi V4 B with a clock frequency of 1.5 GHz is used in the processing of the algorithms. Table VII shows a comparison between the STA/LTA algorithm and the proposed method with respect to the following characteristics: processing time, sample numbers, cumulative time, number of signals and approximate number of basic math operations.

TABLE VII.
EVALUATION OF THE COMPUTATIONAL COST OF ALGORITHMS

Characteristics	***STA/LTA***	***DFT-SVM***
Processing time	0.08 ms	2.4 ms
Sample numbers	2000	200
Cumulative time	20 s	1 s
Number of signal	3	2
Basic mathematical operations	3 addition 8 multiplication	10000 addition 9900 multiplication

IV. CONCLUSIONS

The proposed method detects a motion in the structure equal to or slightly better in time than the STA/LTA algorithm. The thresholds found to recognize a motion are 3 and -2 for the STA/LTA and DFT, respectively. The proposed features and constrains allow us to distinguish between seismic motions and other types of disturbances. Therefore, if the proposed constrains is met, then the alarm is on for this seismic motion. This result is obtained in the first second after the P wave signal appears, which has a correlation with the maximum absolute value of the PGA of the signal. It should be noted that the PGA takes place several seconds after qualifying. For this reason, an imminent danger can be detected seconds before the PGA of the earthquake in the building.

Although the STA/LTA algorithm is 30 times faster in processing time, the proposed methodology only uses one tenth of the data of the STA/LTA algorithm. Therefore, it is more suitable to use the proposed method in microcontrollers with low memory capacity. In addition, this methodology uses one second of cumulative time before processing.

V. ACKNOWLEDGMENT

The authors thank the Centro Peruano Japonés de Investigaciones Sísmicas y Mitigación de Desastres (CISMID) and Instituto Nacional de Investigación y Capacitación en Telecomunicación - Universidad Nacional de Ingeniería (INICTEL-UNI) for the support provided.

REFERENCES

[1] USGS (2022, October 15). Earthquake Hazards. [Online]. Available: https://earthquake.usgs.gov/earthquakes/map/

[2] M. D. Kohler, E. S. Cochran, D. Given, S. Guiwits, D. Neuhauser, I. Henson, R. Hartog, P. Bodin, V. Kress, S. Thompson, et al., "Earthquake early warning shakealert system: West coast wide production prototype," *Seismological Research Letters*, vol. 89, no. 1, pp. 99–107,2018.

[3] C. Peng, P. Jiang, Q. Chen, Q. Ma, and J. Yang, "Performance evaluation of a dense mems-based seismic sensor array deployed in the Sichuan-Yunnan border region for earthquake early warning," *Micromachines*, vol. 10, no. 11, p. 735, 2019.

[4] Y. Kodera, "Real-time detection of rupture development: Earthquake early warning using p waves from growing ruptures," *Geophysical Research Letters*, vol. 45, no. 1, pp. 156–165, 2018.

[5] V. K. Chauhan, K. Dahiya, and A. Sharma, "Problem formulations and solvers in linear svm: a review," *Artificial Intelligence Review*, vol. 52, no. 2, pp. 803–855, 2019.

[6] M. Ebrahimi, A. Moradi, M. Bejvani, and M. Davatgari Tafreshi, "Application of sta/lta based on cross-correlation to passive seismic data," in *Sixth EAGE Workshop on Passive Seismic*, vol. 2016, pp. 1–5, EAGE Publications BV, 2016.

[7] S. A. Veluthedath Shajihan, R. Chow, K. Mechitov, Y. Fu, T. Hoang, and B. F. Spencer Jr, "Development of synchronized high-sensitivity wireless accelerometer for structural health monitoring," *Sensors*, vol. 20, no. 15, p. 4169, 2020.

[8] F. Di Nuzzo, D. Brunelli, T. Polonelli, and L. Benini, "Structural health monitoring system with narrowband iot and mems sensors," *IEEE Sensors Journal*, vol. 21, no. 14, pp. 16371–16380, 2021.

[9] InvenSense (2013, Augost 19). MPU-6000 and MPU-6050 Product Specification Revision 3.4 [Online]. Available: https://invensense.tdk.com/wp-content/uploads/2015/02/MPU-6000-Datasheet1.pdf

[10] Raspberry Shake (2021, Febrary 1). Specifications for: Raspberry Shake RS4D [Online]. Available: https://manual.raspberryshake.org/_downloads/SpecificationsforRaspberryShake4DMEMSV4.pdf

[11] E. Del Valle, R. Meli, O. Rascón, E. Bazán, and O. De Buen, *Diseño sismico de edificios*. 2003.

[12] CEOIS (2022, July 3). Centro de Observación para la Ingeniería Sísmica del CISMID-FIC-UNI [Online]. Available: http://www.cismid.uni.edu.pe/ceois/red/

[13] Solidworks (2022, July 3). Dassault Systèmes SolidWorks Corporation [Online]. Available: https://www.solidworks.com/es

[14] A. K. Chopra, *Dynamics of structures*. Pearson Prentice Hall Hoboken, 2014.

[15] A. Arias, "Measure of earthquake intensity.," pp 438-83 of *Seismic Design for Nuclear Power Plants. /Hansen, Robert J.* (ed.). Cambridge, Mass. Massachusetts Inst. of Tech. Press (1970).

[16] A. Blakeborough and M. Williams, "Measurement of floor vibrations using a heel drop test," *Proceedings of the Institution of Civil Engineers Structures and Buildings*, vol. 156, no. 4, pp. 367–371, 2003.

[17] A. V. Oppenheim, R. W. Schafer, J. R. Buck, et al., *Tratamiento de señales en tiempo discreto*. Pearson Educación, 2011.

[18] G. James, D. Witten, T. Hastie, and R. Tibshirani, *An introduction to statistical learning*, vol. 112. Springer, 2013.

[19] E. A. T. Loza, A. C. Nieto, and S. G. H. Bustamante, "Accelerometer prototype with combined filtering for noise attenuation using an embedded system and low-cost mems sensors for building monitoring," in *2022 IEEE XXIX International Conference on Electronics, Electrical Engineering and Computing (INTERCON)*, pp. 1–4, IEEE, 2022

[20] Shinken (2022, July 3). Series Vibration Test Systems [Online]. Available: https://www.shinken-ltd.co.jp/cms/wp-content/themes/shinken_ver1.2/pdf/en/3_G-0_2.pdf.